Highly conductive mixed PEO/PAN based membranes for solid state Li Ion batteries via electro spinning and hot press synthesis routes

Robert J. Spranger, Leo van Wüllen, Anna Kirchberger, Tom Nilges

Angaben zur Veröffentlichung / Publication details:

Spranger, Robert J., Leo van Wüllen, Anna Kirchberger, and Tom Nilges. 2026. "Highly conductive mixed PEO/PAN based membranes for solid state Li Ion batteries via electro spinning and hot press synthesis routes." *Zeitschrift für anorganische und allgemeine Chemie* 652 (2): e202500062. https://doi.org/10.1002/zaac.202500062.

Journal of Inorganic and General Chemistry
ZAAC
Zeitschrift für anorganische und allgemeine Chemie
www.zaac.wiley-vch.de
RESEARCH ARTICLE
Check for updates
DOI: 10.1002/zaac.202500062

Highly-Conductive Mixed PEO/PAN-Based Membranes for Solid State Li-Ion Batteries via Electro-Spinning and Hot-Press Synthesis Routes

Robert J. Spranger, Leo van Wüllen,* Anna Kirchberger, and Tom Nilges*

Polyethylene oxide (PEO)-based solid polymer electrolytes (SPEs) have been extensively studied for all solid-state batteries (ASSBs) but still suffer from low thermal stability and ionic conductivity. Here, we report on PEO-based solid electrolytes containing a second polymer, polyacrylonitrile (PAN) and succinonitrile (SN). Two different synthesis routes have been followed, synthesis via hot-pressing and synthesis via electrospinning. Whereas the hot-pressing route offers a well-established and robust approach without the need of using solvents, electrospinning provide samples with a distinctively superior performance as compared to those prepared via solution casting. Both routes resulted in materials exhibiting an ionic conductivity around 10^{-4} S cm^{-1} at room temperature. Using solid-state NMR approaches, we could show that SN increases the chain segment mobility of PEO and hence supports Li mobility, whereas PAN remains virtually immobile. Using a deuterated sample d_4-SN dipolar NMR experiments (^{7}Li-^{1}H-REDOR) at 190 K revealed that the coordination of the Li cations within the mixed polymer electrolytes in solely accomplished by the polyether functionalities without the help of SN. The addition of PAN seems to increase the relative amount of amorphous PEO, hence supporting the overall Li mobility, and it increased the mechanical stability of the membranes.

1. Introduction

The ever increasing demand for battery systems for high power lithium ion batteries (LIBs) for automotive transportation still constitutes an important challenge in materials science. Today's LIB technology still mostly relies on the use of liquid electrolytes—a Li salt dissolved in a set of organic aprotic solvents such as propylene carbonate (PC), dimethyl carbonate (DMC) or ethylene carbonate (EC)—mainly due to the high ionic conductivity in liquid electrolytes. Several issues connected to the use of liquid electrolytes, including battery safety, possible leakage, and limited energy density, has shifted the focus to the development of solid-state electrolytes to minimize these limitations.[1–3] A quite demanding property profile—high ion conductivity, mechanical and thermal stability, a large electrochemical window, and environmental compatibility—has to be met by a successful candidate. Various classes of solid electrolytes have been explored, ranging from crystalline electrolytes and glasses to glass-ceramic-based and solid polymer electrolytes.[4,5] The latter offer the advantage of high mechanical flexibility, ease of processability and reduced weight.[6–9] The increased mechanical flexibility of SPEs enables their use in a multitude of electrical cell constructions.[10] This flexibility allows for the possibility of smaller, lighter, safer cells that offer higher energy densities, enhanced cycle stability, and the potential for flexible geometries.[11]

Building on the pioneering work of Armand and Wright,[12–14] who first demonstrated that poly(ethylene oxide) (PEO) could effectively dissolve lithium salts through coordination of lithium cations with the ether oxygen atoms, significant research has focused on optimizing lithium ion conductivity. Their discovery that the ion conductivity in these systems is closely linked to the segmental dynamics of the PEO chains in the amorphous regions has prompted extensive efforts to enhance this property. Consequently, considerable attention has been devoted to identify potential additives, such as plasticizers or fillers, that could address this challenge. A number of studies have been conducted on the use of fillers to enhance the conductivity of polymer electrolytes, with a particular focus on materials such as TiO_2, Al_2O_3, or SiO_2.[15–17]

Rather encouraging results have been achieved using succinonitrile (SN) as a solid lubricant which enhances the PEO segmental mobility. However,[18,19] it was found that the amount of SN (PEO/SN ratio < 1) needed to achieve high ionic conductivity heavily deteriorated the mechanical stability of the membranes which are usually fabricated via a solution casting process. In recent articles, we could show that electrospinning as an alternative synthesis route presents a promising alternative

R. J. Spranger, L. van Wüllen
Institute of Physics, University of Augsburg
Universitätsstraße 1, 86159 Augsburg, Germany
E-mail: leo.van.wuellen@physik.uni-augsburg.de
A. Kirchberger, T. Nilges
Chemistry Department, Technische Universität München, Lichtenbergstr. 4, 85748 Garching bei München, Germany
E-mail: tom.nilges@tum.de
A. Kirchberger
TUMint.Energy Research GmbH, Lichtenbergstr. 4, Lichtenbergstraße 4, 85748 Garching bei München, Germany

Supporting information for this article is available on the WWW under https://doi.org/10.1002/zaac.202500062

to solution casting techniques. With a PEO/SN ratio of 0.25, SPEs with high ionic conductivities $>10^{-4}$ Scm^{-1} at room temperature were successfully prepared.

Despite all this promise, the low melting point of PEO of about 55 °C limits the mechanical and thermal stability of the membranes. Here, the addition of a second polymer such as polyacrylonitrile (PAN) with a decomposition temperature of 280 °C may prove advantageous. Contrasted to PEO, PAN does not exhibit segmental chain mobility and thus cannot support Li transport but has been shown to serve as a hosting matrix in PAN:SN:LiX systems in which Li cations are transported across the matrix as $Li^+(SN)_x$ moieties.[20] Adding PAN to a PEO:SN:LiX system may thus not only entail a decrease in the amount of crystalline PEO and an increase in the mechanical and thermal stability but also provide additional Li migration pathways. We note that the use of mixed polymer PEO/PAN systems as electrolyte materials has been attempted;[18,21–24] however, the residual solvent content was rather high, the material thus more resembling a gel electrolyte.

In this work, we present an in-depth study of solid electrolytes in the multinary system PEO:PAN:SN:$LiBF_4$. Since in previous work by us we noticed a partial loss of SN during the synthesis route via electrospinning, we evaluated whether the ES protocol (with the necessity of producing a homogeneous solution of all ingredients in the first place) is suitable for the synthesis of these multinary systems. As a second route, we followed the established solvent-free hot-pressing method.[25–28]

With both routes membranes exhibiting room temperature ion conductivities of approx. 10^{-4} S cm^{-1} could be produced. The influence of the PEO/plasticizer and PEO/PAN ratio on the Li cation and PEO segmental mobility was studied applying a range of solid-state NMR approaches including temperature dependent static ^{7}Li and ^{19}F NMR spectroscopy, ^{13}C-MAS (Magic Angle Spinning), and CP-MAS (cross polarization) NMR spectroscopy. In this study, the focus lies on the investigation of the local ion dynamics and conductivity dependence on the preparation process of the SPEs rather than its application in battery systems. Selected PEO/PAN systems were subject to such investigations and results are reported elsewhere.[29]

2. Results and Discussion

This section commences with a presentation and discussion of the sample compositions as determined via the analysis of the solid-state ^{13}C MAS NMR and liquid state ^{1}H NMR spectra and a comparison of the morphology of the ES and HP samples. Subsequently, further experimental results on ES and HP samples will be given separately.

2.1. Sample Compositions

In previous works (PEO:SN:MX samples, M = Na, Li, X = CF_3SO_3, BF_4),[17,30,31] the SN content of the ES samples was occasionally found lower than the nominal values. Since the current system even shows a higher complexity, it seems mandatory to check the compositions of the synthesized ES samples to assess the reproducibility of the ES method. These were determined using two different NMR approaches: a) analysis of ^{13}C-MAS spectra recorded with high power proton decoupling and b) analysis of liquid state ^{1}H-NMR spectra on samples dissolved in DMSO-d6. Details of the procedure are given in the supporting information. The resulting compositions are presented in **Table 1** for a batch of five samples of the same target composition. Whereas the relative fraction of the two different polymers PEO and PAN is found to be quite consistent, thus reproducible, across the investigated samples, quite heavy variations are found in the content of SN and PC, both added as plasticizers. Especially PC seems to be virtually lost during the synthesis and drying process, except for sample ES1. Since the presence of the plasticizers has been found to be rather important to boost the ionic conductivity in PEO- and PAN-based polymer electrolytes,[30–32] this may counterbalance the positive effect of ES morphology on the key property of the material,[30,31] Li ionic conductivity (vide infra). While these results emphasize that the synthesis of these multinary complex polymer electrolytes is principally possible using the ES technique, maintaining constant compositions and hence properties seems to be extremely difficult. Interestingly, some samples (especially ES1 and ES4) contain significant amounts of DMSO, used as solvent.

Table 1. Compositions of a set of batches of ES samples of nominally identical composition as determined from a deconvolution of the ^{13}C-MAS NMR spectra, recorded with high power proton decoupling (SS-NMR), and a deconvolution of ^{1}H liquid-state NMR spectra.

		Molar ratio					
Batch number	Method	PEO	PAN	SN	PC	DMSO	$LiBF_4$
Target	–	10	8	5	4	–	1
ES1	SS-NMR	10	14	6	2	7	–
	LS-NMR	n.m.	–	–	–	–	–
ES2	SS-NMR	10	12	1	0	0	–
	LS-NMR	10	10	0.5	0	–	–
ES3	SS-NMR	10	13	0.5	0	0	–
	LS-NMR	10	10	0.5	0	–	–
ES4	SS-NMR	10	9	4	0.5	3	–
	LS-NMR	10	10	3	–	–	–
ES5	SS-NMR	10	11	4	0	2	–
	LS-NMR	10	15	4	–	–	–

Contrasted to this, the determined compositions for the samples prepared via hot-pressing are found quite near to the nominal compositions, as shown in **Table 2**. Notably, no significant loss of SN could be observed. Thus, this synthesis route proves more robust as compared to ES for the preparation of complex, multinary polymer electrolytes. Another important point are the mechanical properties of the hot-pressed systems. The mechanical behavior strongly depends on the composition of the samples.

2.2. Morphology

The morphology of the electro-spinning and hot-pressed samples was examined using scanning electron microscopy (SEM), with the results for two exemplary samples (ES1 and HP1) presented in **Figure 1**. Whereas the ES sample displays an interwoven fiber structure, resulting in a woven membrane, no such fiber structure is visible for the HP sample, which is characterized by extended melt like regions. The diameters of the fibers in the ES sample are predominantly found within the range of 0.5 to 10 μm, however with an overall broad distribution with the largest diameters of up to 40 μm. It is this fibrous structure of the ES samples which has been found to facilitate conductivity in PEO-based systems.[30,31]

2.3. Results on Samples Synthesized via Electrospinning

In response to the difficulties in maintaining constant compositions with respect to the plasticizer contents and hence properties, we restricted our analysis of the samples synthesized via electrospinning to the five batches as mentioned above without an attempt to study the influence of variations in the compositions of the membranes (PAN/PEO ratio, PEO/plasticizer ratio) on the performance of the membranes. As soon as a reliable synthesis protocol is at hand, we will return to this important point.

Table 2. Determined composition of the quantitative evaluation of the ^{13}C-MAS spectra with high power proton decoupling and ^{1}H liquid-state NMR spectra of the system PEO:PAN:SN:$LiBF_4$.

			Molar ratio			
Batch number	Target composition (molar ratio)	Method	PEO	PAN	SN	$LiBF_4$
HP1	18:18:9:1	SS-NMR	18	16	9	–
		LS-NMR	18	21	10	–
HP2	18:18:6:1	SS-NMR	18	16	6	–
		LS-NMR	18	22	7	–
HP3	18:18:3:1	SS-NMR	18	16	3	–
		LS-NMR	18	19	3	–
HP4	18:18:0:1	SS-NMR	18	17	0	–
		LS-NMR	18	19	0	–
HP5	18:6:9:1	SS-NMR	18	4	9	–
		LS-NMR	18	7	12	–
HP6	6:18:9:1	SS-NMR	6	16	9	–
		LS-NMR	6	18	9	–
HP7	18:0:9:1	SS-NMR	18	0	9	–
		LS-NMR	n.m.			
HP8	0:18:9:1	SS-NMR	0	18	11	–
		LS-NMR	0	18	8	–
HP1-d4	18:18:9-d^4:1	SS-NMR	18	20	9[a)]	–
		LS-NMR	n.m.			

[a)]Only the resonance of the nitrile groups was used for the determination.

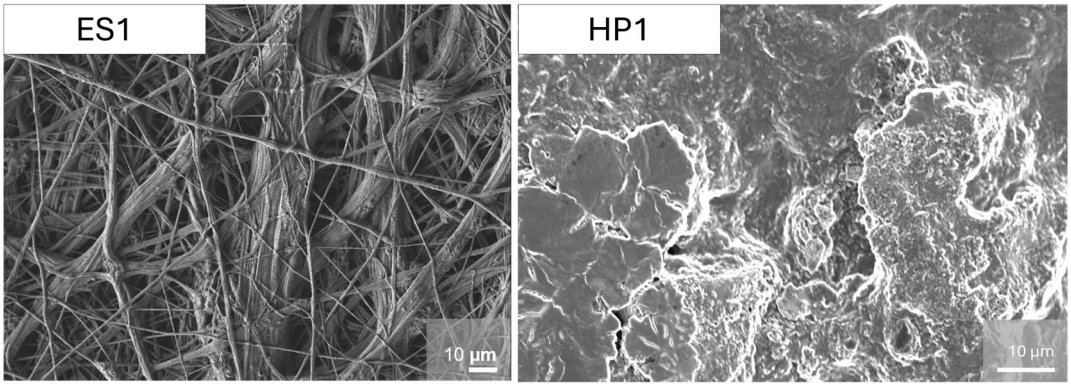

Figure 1. SEM images of the membranes synthesized via electrospinning (left) and hot-pressing (right).

2.3.1. NMR Spectroscopy

The inherent element selectivity of NMR spectroscopy allows to individually study the mobility of the Li cation (^{6,7}Li-NMR), the anion (^{19}F-NMR), and the dynamics of the hosting polymers (^{1}H-NMR, ^{13}C-NMR) and thus offers a wealth of information about the dynamic processes present in the electrolytes. Temperature-dependent static ^{7}Li and ^{19}F single pulse experiments were carried out for samples ES1, ES3, and ES4. The temperature-dependent evolution of the ^{7}Li NMR spectra for sample ES1 is exemplary shown in **Figure 2**a. The plotted spectra represent the central ($m = ½ \leftrightarrow m = -½$) transition of the $I = 3/2$ ^{7}Li nucleus. This transition is independent of the quadrupolar coupling and its line width mainly dominated by the homo- and heteronuclear dipole interaction, the orientational dependence of which is governed by the second Legendrian, $3cos^2\beta - 1$, with β denoting the angle between the applied magnetic field and the principal axis of the dipole interaction tensor. As a consequence, any dynamic process will impart a (partial) averaging of the orientational dependence and thus will lead to a narrowing of the NMR line.

As is obvious from an inspection of Figure 2, there is a clear turnover from a line width of ca. 4800 Hz at low temperatures (which marks the rigid lattice regime) to a narrowed line width of ca. 300 Hz (denoting the extreme narrowing limit) in the temperature range $185\ K < T < 220\ K$, indicating the onset of Li mobility within this temperature range. Taking the temperature for which the observed line is given by $(\upsilon_{rigid\ lattice} - \upsilon_{mot.\ narrowing})/2 + \upsilon_{mot.narrowing}$ as the onset temperature ($T_{onset}(ES1) = 204$ K) and using the empirical Waugh-Fedin relation $E_A = 0.156 \times T_{onset}$ [33] allows for a rough estimate of the activation energy for Li mobility, which in this case is calculated as $E_A = 32$ kJ mol^{-1}. For samples ES3 and ES4, the onset temperatures and activation energies as determined from the evolution of the line width with temperature are $T_{onset} = 259$ K, $E_A = 40$ kJ mol^{-1} and $T_{onset} = 223$ K, $E_A = 35$ kJ mol^{-1} for ES3 and ES4, respectively. The evolution of the ^{19}F line width with temperature closely follows that of the corresponding ^{7}Li line, only slightly shifted to higher temperatures. This is due to the fact that for line narrowing the correlation time of the motional process has to exceed the inverse of the corresponding NMR line width, which is much larger for ^{19}F (^{19}F-FWHH(ES1) = 11.8 kHz and ^{7}Li-FWHH(ES1) = 4.8 kHz at T = 180 K).

In view of the determined sample compositions as given above (Table 1), a clear correlation between the amount of plasticizer (SN + PC) and ion mobility (Li cation, BF_4 anion) mobility is observed. Sample ES1, containing the largest amount of plasticizers, plus a considerable amount of DMSO used as solvent, shows the by far highest Li mobility with an onset temperature of 204 K, for sample ES3, containing hardly any plasticizer, the temperature is shifted to 259 K.

The onset temperature for sample ES4 is comparable to those found for electrospun samples in the systems PEO:SN:$LiBF_4$ [31] PEO:SN:$NaBF_4$ [30] and PEO:SN:LiTFSI [32] and may be traced back to the action of SN as a solid lubricant, i.e., to activate and enhance the segmental chain mobility of the PEO chains which then supports ion conductivity at temperatures above the phase transition of SN. For sample ES1, however, due to the presence of a second polymer species (PAN) and the considerable amounts of SN and PC (and in addition DMSO), it is not possible to clearly conclude which ingredient is responsible for the remarkable Li mobility even at temperatures distinctively below the SN phase transition. Considering the large amounts of PC and DMSO present in the sample, formation of $Li(PC)_n$ couples or the action of PC as a solid plasticizer for an enhancement of the chain mobility may also be present. Further, the phase transition of SN may be shifted to lower temperatures in this multinary mixture (vide infra). In addition, the presence of PAN may also change the PEO chain mobility and thus indirectly influence Li mobility within these sample. However, this seems rather improbable in view of the comparable PAN/PEO ratios of the investigated samples.

It is interesting to check whether the observed drastic changes in ion mobility, depending on the amount of (SN + PC) in the samples, is correlated to the mobility of the PEO chains. This can be evaluated using ^{13}C MAS NMR spectroscopy. As shown, e.g., in,[18,19,30,31] the presence of SN in PEO-based

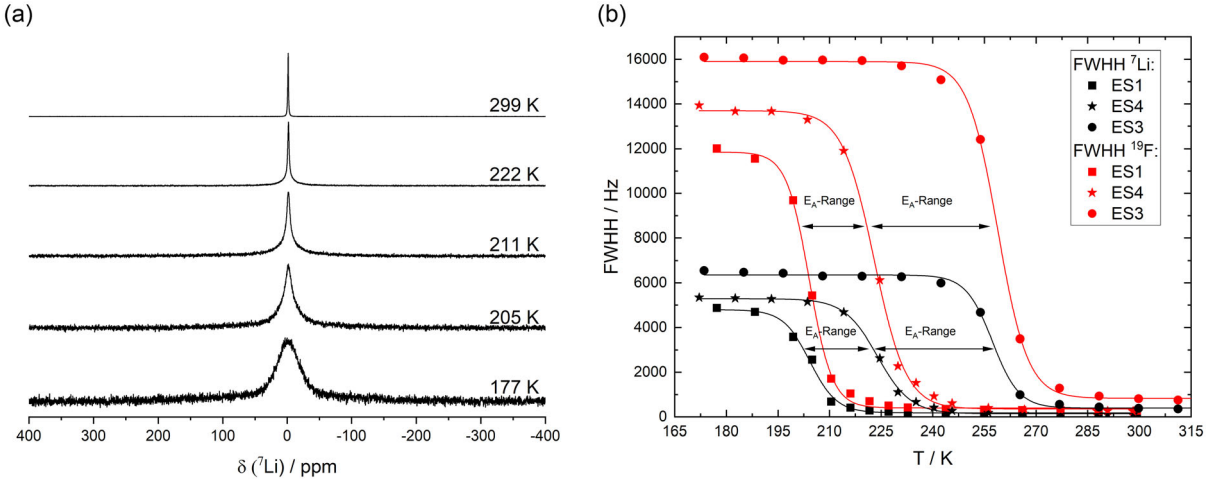

Figure 2. a) Temperature-dependent static ^{7}Li spectra of ES1 and b) the evolution of the ^{7}Li and ^{19}F line width as a function of temperature for three batches of PEO/PAN:SN/PC:$LiBF_4$ membrane. Line to guide the eye.

systems may impart a drastic increase in the mobility of the PEO matrix, acting as a solid lubricant. This extremely high mobility manifests itself in the occurrence of a triplet of the ^{13}C PEO signal (methylene groups) around 70 ppm (acquired without ^{1}H decoupling) due to the ^{1}J-($^{13}C^{1}H$)- coupling to the methylene ^{1}H nuclei.

The corresponding ^{13}C-MAS-NMR spectra, taken at room temperature and acquired without ^{1}H decoupling, are collected in Fig. S2a. Up to five different (sets of) signals can be identified. We assign the narrow signal at 156.2 ppm, which is only observed for sample ES1, to PC. The signal around 40 ppm, which is split into a quartet, is indicative of the presence of DMSO in the sample (^{1}J-($^{13}C^{1}H$) coupling constant of 138 Hz). Further signals at 14. 5 ppm (methylene group, split into a triplet) and 119.1 ppm (nitrile group) can be assigned to SN. The dominant signal at 70.1 ppm represents PEO. For samples ES1, ES3, and ES4, this signal exhibits a triplet structure due to the mentioned J(C–H) coupling of 142 Hz, indicating a remarkable PEO chain mobility in these samples. Thus, we observe that the cation mobility as discussed above seems to be highly correlated to this chain mobility and the overall plasticizer content of the samples. We note that under the experimental conditions (no ^{1}H decoupling), the ^{13}C MAS NMR signals of PAN are too broad to be resolved; these are only observable under strong ^{1}H decoupling (cf. Fig. S2b, supporting information). The same holds for any fraction of PEO not involved in this extreme dynamics (vide infra, **Table 3**). Since the CSA parameters of the nitrile resonance at 120.5 ppm (width = 496 Hz, $\Delta\sigma$ =-196 ppm, $\eta_{CSA} = 0.27$) are virtually identical to those of pristine PAN, PAN in the membranes may be viewed as more or less immobile within the membranes, as in the case of PEO:SN:$LiBF_4$ samples synthesized via solution casting.[20]

2.3.2. Impedance Spectroscopy

In addition to the detailed solid-state NMR study as presented above, Li mobility was also checked using potentiostatic electrochemical impedance spectroscopy. The temperature-dependent conductivities are plotted in **Figure 3**. Interestingly, no large variation in the ionic conductivities are found across the various samples; the room temperature conductivities are found around 10^{-4} Scm^{-1}, with the exception of sample ES5 (0.2×10^{-4} Scm^{-1}). Activation energies vary drastically between 25 and 118 kJ mol^{-1} with no clear correlation to synthesis, compositional, or morphology parameters. Therefore, an interpretation of these results was not attempted. These results are clearly at variance with the results from the solid-state NMR analysis outlined above and do not fit the general trend that an increased amount of plasticizer will lead to an increase in ionic conductivity. At this point in time, we do not have any explanation for this observation.

While no quantitative mechanical characterization of the ES PEO/PAN electrolyte was conducted within this study, several qualitative observations can be reported based on the membrane fabrication and handling. Electrospinning of a pure PAN electrolyte according the mentioned ES protocol is possible but the resulting fibrous membrane still tended to fragment or splinter during handling. Upon introducing PEO into the PAN system (via electrospinning), the flexibility of the membranes improved markedly. The PEO/PAN composite membranes exhibited significantly better mechanical integrity and processability, allowing for easier cutting and manipulation without fracture.

As stated above, these results indicate that it is indeed possible to synthesize membranes with very high Li mobility following the ES approach. One of the advantages of this process is its ability to virtually fully suppress the crystallization of PEO, as no PEO reflexes are found in the XRDs (data not shown). As the Li migration predominantly occurs within the amorphous parts of PEO, this marks a clear advantage of this synthesis route. However, it turned out that it is extremely difficult to control all synthesis and post processing parameters to maintain constant composition and hence properties. We are currently trying to develop a synthesis protocol which guarantees reproducible compositions which then will be the entry point for a further in depth investigation of the effect on composition, synthesis, and processing parameters on the performance of the membranes.

2.4. Results on Samples Synthesized via Hot-Pressing

As described in the previous section, for the hot-pressed membranes, the actual determined compositions were always found to be close to the target compositions (Table 3). Therefore, a detailed investigation of the influence of the composition on the materials' properties was conducted, the results of which are presented in the following.

2.4.1. X-Ray Diffraction

X-ray diffractograms for the samples synthesized via hot-pressing are collected in **Figure 4**. The reflexes at 19.1° and 23.2° are attributed to the crystalline fraction of the PEO phase, whereas the broad reflex at 18.8° can be assigned to PAN. Comparing the

Table 3. Determined proportions of the quantitative evaluation of the ^{13}C-MAS spectra with high power proton decoupling of the amorphous and crystalline phase of the polymer PEO.

Sample	Composition	Amorphous phase in [%]	Crystalline phase in [%]	PEO_3:$LiBF_4$ in [%]
	Pure PEO	6	94	–
HP1	18:18:9:1	100	0	–
HP2	18:18:6:1	80	20	–
HP3	18:18:3:1	45	55	–
HP4	18:18:0:1	[a]–	85	15

[a]Due to the overlapping of the different signals, no percentage could be determined.

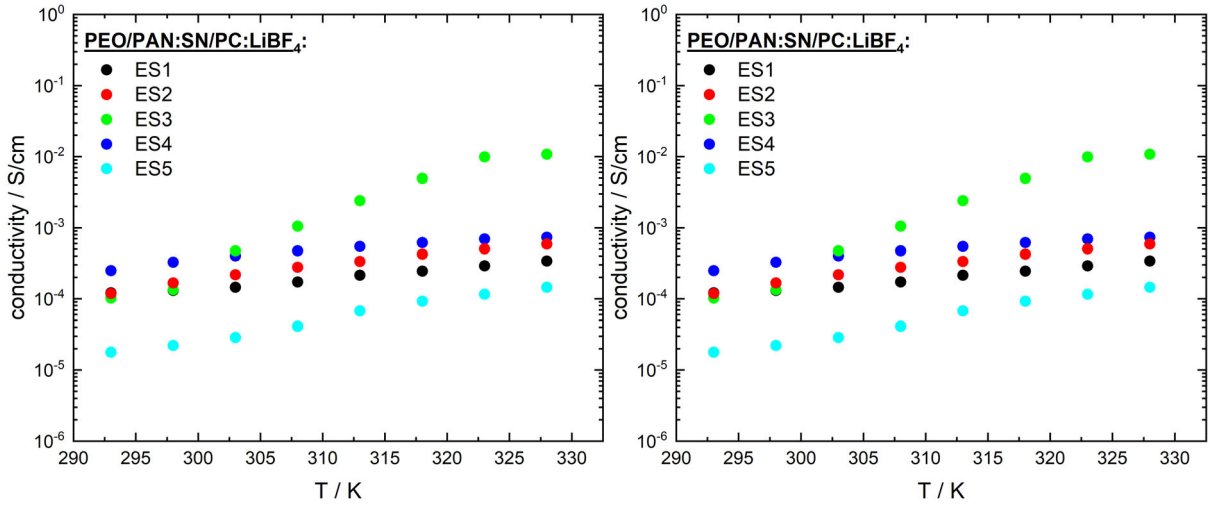

Figure 3. Temperature dependent evolution of the ionic conductivity for the studied ES samples.

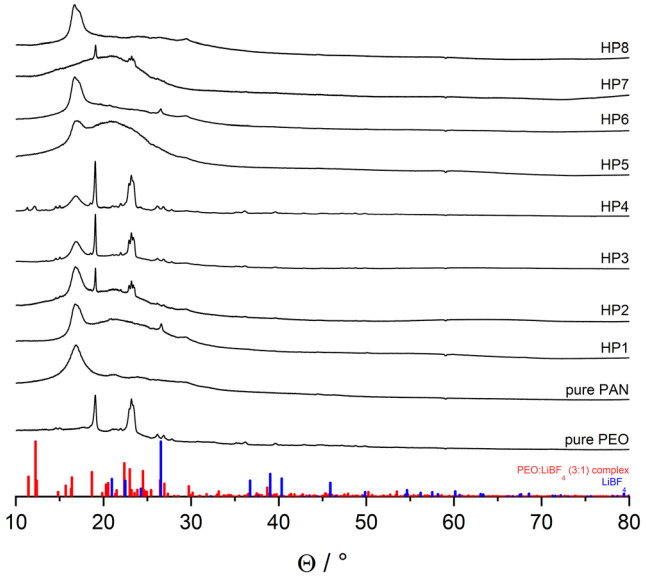

Figure 4. XRD analysis of the HP samples.A decrease of crystallinity with increasing plasticizer amount can be observed. Additionally, the theoretical diffractograms of the pure $LiBF_4$ salt (blue) and the complex (red) are presented.[46,47]

diffractograms for samples HP1 to HP4 (decreasing SN content with otherwise identical composition), it is clear that SN effectively suppresses the crystallization of PEO. In addition, when comparing samples HP1 and HP7 (PAN-free sample), the occurrence of the reflexes attributed to PEO in HP7 indicates that the presence of PAN seems to help in the suppression of formation of crystalline PEO in the membranes. This may be readily explained by the additional disorder inserted into the system by the incorporation of SN and PAN into the system. Another phase which is suppressed by the presence of SN is the crystalline PEO_3:$LiBF_4$ complex. The corresponding reflexes at 12.1° and 11.3° are observable for the SN-poor samples HP3 and HP4.

2.4.2. NMR Spectroscopy

As with the ES samples, solid-state NMR experiments were conducted to obtain information about the dynamic processes present in the electrolyte membranes. The ^{7}Li- and ^{19}F-MAS NMR spectra are given in the supporting information (cf. Fig. S3). With the exception of sample HP4, the ^{7}Li and ^{19}F MAS NMR spectra exhibit narrow signals without sizeable spinning sideband intensity. The chemical shift of the ^{7}Li signals is found around −1.3 ppm, and the shift of the ^{19}F signal around −151.5 ppm. In addition to these, sample HP4 exhibits broad signals at −1.5 ppm (^{7}Li, comprising 80% of the total signal intensity) and −155.5 ppm (^{19}F). Comparing these to the values published in[18], these signals can be assigned to the crystalline PEO_3:$LiBF_4$ complex and thus corroborate the results from the X-ray diffraction analysis. For sample HP8, the PEO-free sample, the position of the ^{7}Li and ^{19}F signals expectedly are well shifted from that of the other samples (^{7}Li: −1.8 ppm, ^{19}F: −153.4 ppm) indicating a different coordination of the Li cations (with PAN or SN instead of PEO).

Data for the temperature dependent evolution of the line widths of the static ^{7}Li and ^{19}F NMR spectra, obtained after single pulse excitation is collected in **Figure 5**. Whereas Figure 5a shows the variation with plasticizer content, Figure 5b highlights the dependence of the PEO/PAN ratio. In the case where multiple ^{7}Li- or ^{19}F-species were identified (sample HP4), only the evolution of the narrow line is represented. Contrasted to the data for the ES samples, a clear correlation is found between the onset temperature (and hence activation energy) and the plasticizer content, increasing from 35 kJ mol^{-1} for HP1 (polymer/plasticizer ratio 4:1) and HP2 (ratio 6:1) to 39 kJ mol^{-1} for HP3 (ratio 12:1) and 42 kJ mol^{-1} for the plasticizer free samples HP4.

As obvious from inspection of Figure 5b, varying the PAN/PEO ratio does not entail any sizeable changes in the ion dynamics. This indicated that the addition of PAN does not deteriorate the Li mobility. Interestingly, the PEO-free sample HP8 exhibits the lowest onset temperature of all samples. As compared to related

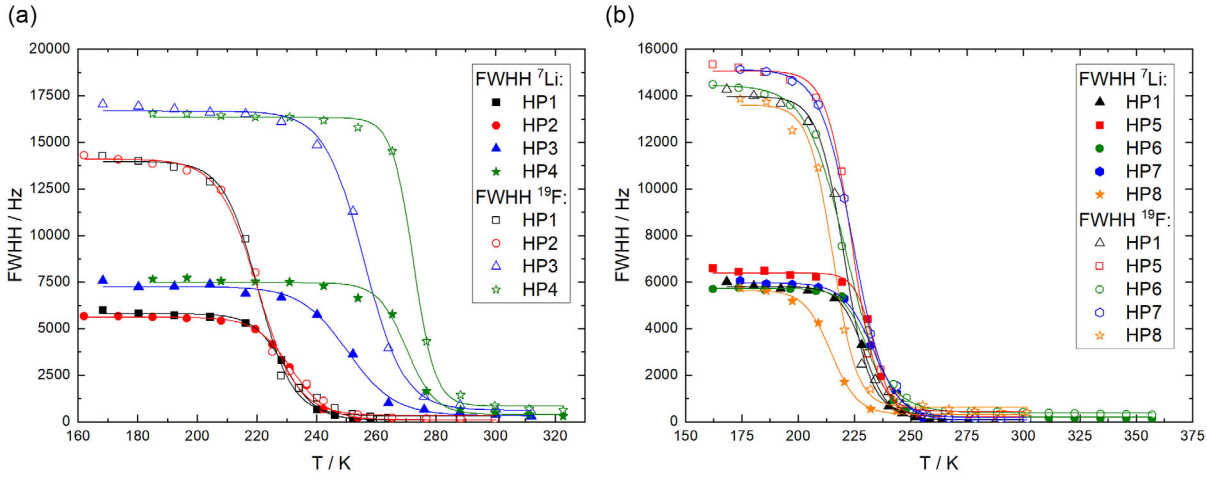

Figure 5. Evolution of the ^{7}Li and ^{19}F line width as a function of temperature for the PEO:PAN:SN:$LiBF_4$ system. a) Variation of the plasticizer amount and b) variation of the PEO/PAN ratios.

samples prepared via solution casting, in which most of the Li cations remained immobile up to temperatures around room temperature,[20] here the complete Li inventory is found mobile at temperatures larger than 225 K. In addition, in[20] a large excess of SN was used. Since in plasticizer-free PAN-based electrolytes hardly any room temperature mobility is found, this has to be ascribed to the formation of $Li(SN)_n^+$ aggregates as found by Voigt et al.[20] In the ^{13}C-MAS NMR spectra, obtained without strong ^{1}H decoupling (cf. Figure S4a), samples HP1- HP3 and HP5—HP7, i.e., those containing PEO and SN, exhibit the triplet pattern for the PEO signal at 70 ppm due to the $^{1}J(^{13}C^{1}H)$ coupling. As with the ES samples, this indicates extremely fast segmental mobility of the PEO chains. We note that in this experiment, signals from immobile PEO or PAN are hardly visible due to the dipolar coupling to ^{1}H. The virtual absence of any PEO signal for HP4 perfectly agrees with the results from above and with the view that SN acts as a solid lubricant enhancing PEO segment mobility which then in turn supports Li mobility. Freezing of the segmental chain mobility in the SN-containing samples occurs around 250 K and manifests itself in a loss of the triplet splitting due to dipolar broadening, as exemplified by the temperature-dependent ^{13}C MAS NMR spectra for HP1, shown in Fig. S4b. This broadening closely follows that of the triplet signal from the methylene SN groups at 14 ppm follows, which supports the assumption that the transition of SN into the plastic crystalline phase triggers the onset of PEO chain mobility.

Since it is generally accepted that Li migration predominantly occurs within the amorphous fractions of PEO,[34] we studied the influence of the PEO/SN and PEO/PAN ratio on this parameter. To this end, ^{13}C MAS NMR with strong ^{1}H decoupling was conducted. The resulting spectrum for sample HP3 is exemplarily shown in Fig. S4c of the supporting information. In order to obtain a reliable deconvolution, we need the chemical shift and line width of the broad contributions to the PEO signal, originating from crystalline PEO. These are readily available since the two contributions to the PEO signals (broad signal at 71 ppm from crystalline PEO, narrow signal at 69.5 ppm from amorphous PEO)[35–37] exhibit a completely different contact time behavior in the ^{13}C CPMAS NMR spectra (cross polarization), as shown in Fig. S5 of the supporting information. The upper spectrum of the inset in Fig. S4c, supporting information, shows an expanded view of the PEO signal region, the lower a ^{13}C CPMAS NMR spectrum for HP3 obtained using a contact time of 100 µs, rendering only the broad signal visible, from which the line position and the width of the broad component may be determined. The resulting fractions are collected in Table 3. The amount of amorphous PEO clearly increases with the plasticizer content and reaches 100% in sample HP1. These results are in perfect agreement with the findings from the X-ray diffraction analysis. Thus, the action of SN within the samples seems to be twofold, acting as a solid lubricant and increasing the amount of the amorphous fraction of PEO. In the case of the SN free sample HP4, no amorphous PEO could be detected. Here, the signal around 70 ppm carries contributions from crystalline PEO and from the crystalline PEO_3:$LiBF_4$ complex.

Although PAN does not directly support ion dynamics in the membranes (as with the ES samples, in the HP samples the CSA of the PAN nitrile resonance resembles that of pristine PAN), it indirectly helps in reducing the amount of crystalline PEO (cf. Fig. S6, supporting information). The amount of crystalline PEO is clearly increasing with decreasing PAN content (samples HP1 (0%), HP5 (10%), and HP7 (23%)). These observations are also consistent with the X-ray diffraction analysis.

All the experimental evidence presented so far for the PEO-containing multinary samples indicate membranes in which PAN mainly serves to enhance dimensional stability of the samples without any participation in Li ion coordination or polymer mobility. In addition, the presence of PAN reduces the relative fraction of crystalline PEO. SN acts twofold, as a solid lubricant to enhance PEO chain mobility and to suppress PEO crystallization. We suggest a Li migration mechanism in which the Li cations are exclusively coordinated by the ether oxygen atoms of the PEO chains without any direct participation of SN. On the other hand, in the PEO-free sample HP8, which exhibits decent Li mobility, Li

migration is probably accomplished by transport of $Li^+(SN)_x$ moieties across the PAN matrix as suggested previously.[20]

In an attempt to check whether in the PEO-containing samples SN is contributing to the coordination of Li cations, we performed ^{7}Li-^{1}H-REDOR experiments on sample HP1 and sample HP1-d4, which is a sample with identical composition as compared to HP1 but synthesized using fully deuterated (d4) SN. If SN would contribute significantly to the coordination of Li in the samples, then the REDOR effect should be smaller in the deuterated sample. We note that we did not consider PAN as a potential candidate for Li coordination in view of the results presented in this and related work.[19,20] ^{7}Li-{^{1}H}-REDOR experiments were performed at low temperatures (190 K) to exclude any dynamics which would average the dipolar couplings. Due to the expected strong ^{7}Li-^{1}H dipolar coupling (coordination of Li via the ether oxygens of PEO), we used the constant time variant of REDOR[38,39] for this experiment, keeping the dipolar evolution time constant at two rotor cycles and incrementing the pulse length of the dephasing pulse from 0 to 2π. The data for the sample containing fully deuterated SN-d4 (HP1-d4) and for the corresponding nondeuterated samples (HP1) are collected in **Figure 6**a. Both CT-REDOR curves exhibit the same behavior, revealing a ^{7}Li-^{1}H dipolar coupling of 2200 Hz, based on SIMPSON simulations assuming a two spin interaction. Without attempting to deduce internuclear distances, this marks quite a high value for the dipolar coupling, and, more importantly, no difference is observed between the deuterated and nondeuterated sample. The fact that the removal of protons from SN did not entail any changes in the strength of the dipolar coupling between ^{7}Li and ^{1}H suggests that SN is indeed not participating in the coordination of the Li cations.

This view is supported by a comparison of the ^{7}Li MAS NMR spectra for sample HP1, obtained with and without strong ^{1}H-decoupling, as shown in Figure 6b. For the spectrum obtained with decoupling, the line width considerably narrows to roughly 1/12th of the line width of the nondecoupled spectrum. Moreover, if two distinctively different coordination motifs were present, we would expect the contribution of two ^{7}Li signals to the spectrum, which is not the case. As for sample HP8, a contribution from water to the Li coordination and mobility has to be excluded. To this end, the ^{1}H MAS NMR spectrum of HP8 was analyzed (cf. Fig. S7, supporting information). There is indeed a very tiny signal at 5.3 ppm which we may assign to H_2O, however, with an overall contribution of 0.2% to the total signal intensity this would translate into 0.2 H_2O molecules per Li cation. Thus, also trace amounts of water are present in the sample, the amount is clearly not enough to account for the observed Li mobility.

2.4.3. Impedance Spectroscopy

As with the ES samples, the ionic conductivity and activation energies of the hot-pressed samples was determined using impedance spectroscopy (**Figure 7**). As for the samples HP1—HP4 (decreasing SN content), a clear correlation between SN content and ionic conductivity is observed. Whereas the SN rich compositions HP1 and HP2 exhibit room temperature conductivities around of 10^{-4} Scm^{-1}, the value is decreasing to approx. 10^{-5} Scm^{-1} for HP3 and drops below the detection limit for the SN free sample HP4. Activation energies vary between 29 and 44 kJ mol^{-1} in good accordance with the results from NMR spectroscopy (35 to 42 kJ mol^{-1}). Variations in the relative amount of PAN and PEO on the other hand are found to only exhibit a rather marginal effect. Thus, a reduction of the amount of PAN (HP1, HP5, HP7) is found to only exhibit marginal effects on the ionic conductivity, as exemplified by the data in Figure 7b. Room temperature conductivities slightly above 10^{-4} Scm^{-1} are found for the samples with the only

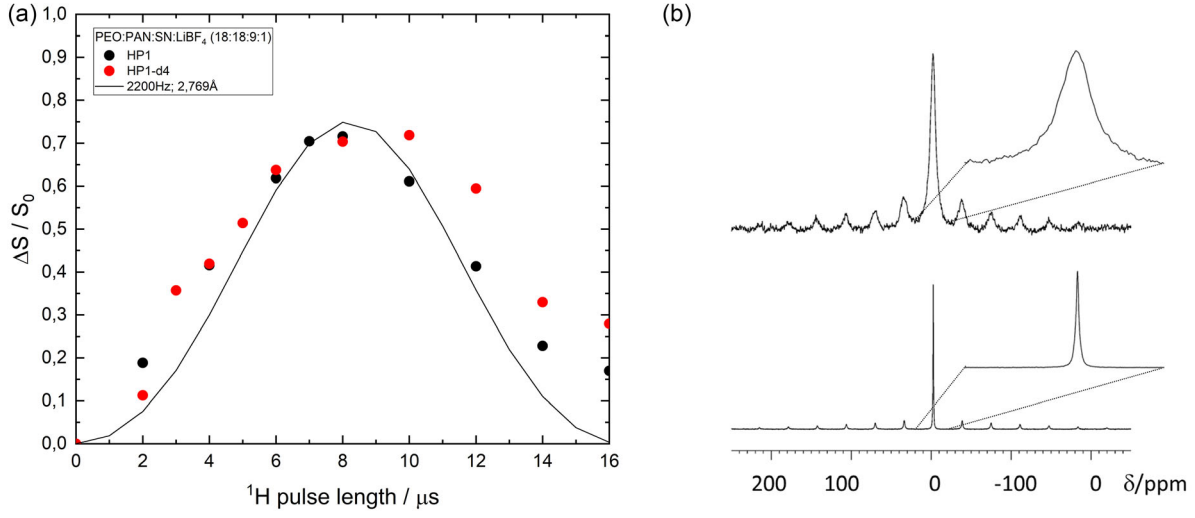

Figure 6. a) ^{7}Li-^{1}H-CT-REDOR data for the nondeuterated (full black circles) sample HP1 and the deuterated (full red circles) sample HP1-d4 (PEO:PAN:SN:$LiBF_4$ 18:18:9:1) at 190 K. The solid line represents the result of a SIMPSON simulation assuming a two spin interaction with D = 2200 Hz). Since the relative ratio of PEO:$LiBF_4$ is 9:1, we do not expect all PEO units to participate in the coordination; thus, the $\Delta S/S_0$ values may be biased to lower values. b) ^{7}Li-MAS NMR spectrum for sample HP1 acquired with (lower spectrum) and without (upper spectrum) strong ^{1}H decoupling.

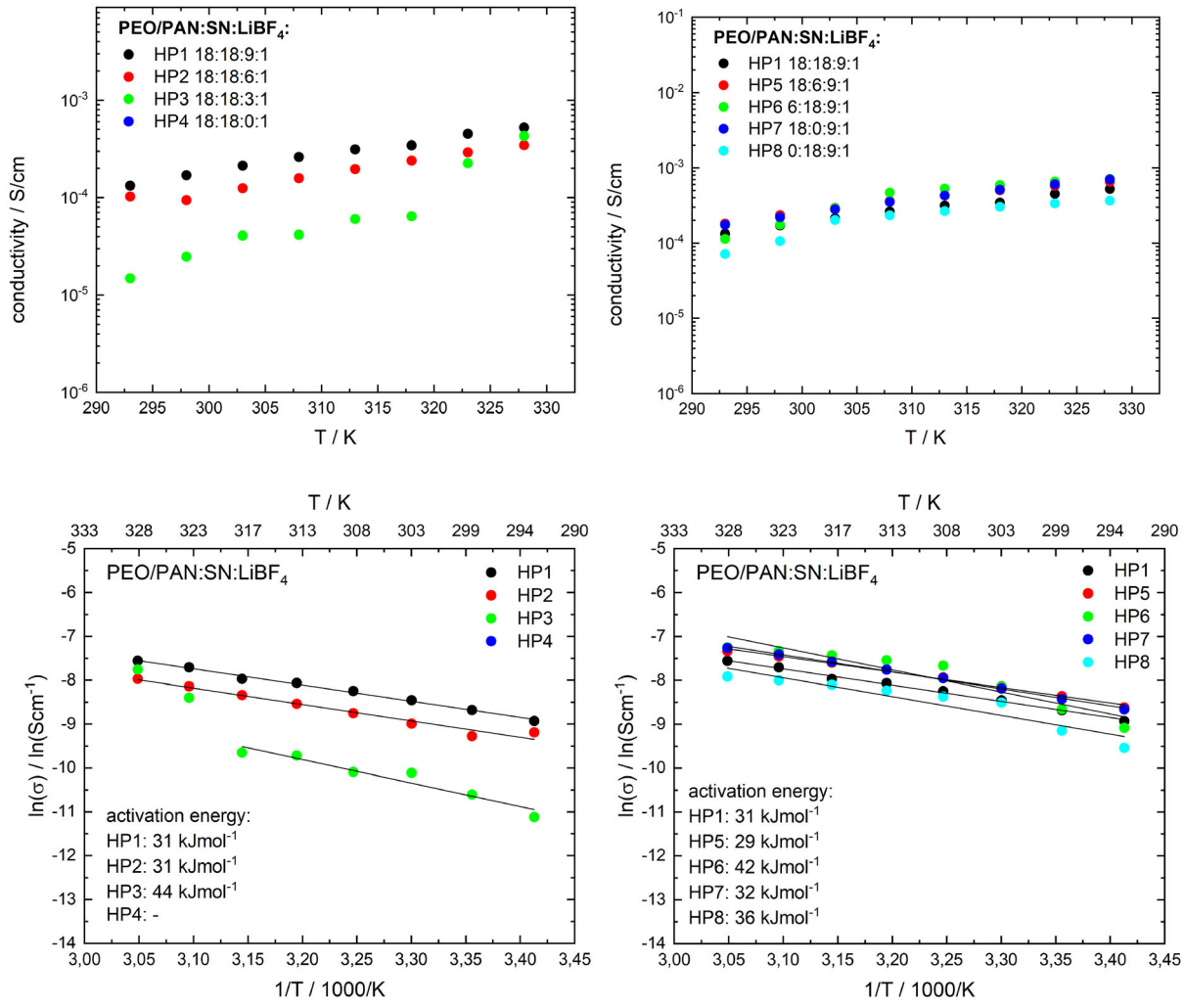

Figure 7. Top: Temperature-dependent conductivity of the variation of plasticizer amount from 18:9:1 to 18:0:1 (left) and variation of the polymer ratio (right). Bottom: Overview of the Arrhenius behavior and the evaluated activation energies of the variation of plasticizer amount from 18:9:1 to 18:0:1 (left) and variation of the polymer ratio (right).

exception of HP8, the PEO-free sample. This indicates that PAN itself is not directly participating in the Li migration process in these samples (in excess of suppressing PEO crystallization). Li migration seems to be correlated to the PEO segmental dynamics (which in turn depends on the SN content), as corroborated by the NMR results presented above. Of course, the PEO-free sample marks an exception. Here, the mechanism of Li transport has to be a different one, e.g., via the formation of $Li^{+}(SN)_x$ species as found in previous work on related compositions prepared via the solution casting process.[20]

Another important point are the mechanical properties of the hot-pressed systems. The mechanical behavior strongly depends on the composition of the samples. Whereas PEO rich membranes proved to be flexible, the incorporation of PAN increased the brittleness. PAN-free membranes with added SN were observed to be rather soft and sticky without being dimensionally stable, whereas PEO-free membranes were dimensionally stable but lacked flexibility. However, the combination of PAN and PEO with SN entailed dimensionally stable, flexible membranes.

In order to set the present study into a broader context, it is important to verify the ion conductivity of the title systems in relation to known polymer electrolytes. Due to the manifold possibilities to create polymer electrolytes, one first has to differ gel (GPE), solid (SPE), and composite polymer electrolytes (CPE). GPEs contain a polymer matrix swollen in liquid electrolyte. SPEs are 'dry' solvent-free systems without organic or ionic liquids where ion transport is realized via the solid phase. CPEs are systems using techniques like polymer blending, cross-linking polymer matrices, binary salt systems, incorporation of additives, doping of nanomaterials, impregnation with ionic liquids, or reinforcement by inorganic fillers to overcome drawbacks from aforementioned systems. Nice review articles reflect this issue.[6,40] Recent developments in PAN-based polymer electrolytes were reviewed by *Whba* et al.[41] where the focus was on PAN systems. An intensively examined field is the modification of pure PEO by blending, copolymerization, and doping with inert (mostly metal oxides) and active (ion conducting active materials) additives.[42]. It has to be stated at this point that the selected samples in **Table 4**

Table 4. Overview of various PEO/PAN polymer electrolytes. Conductivities are denoted at room temperature unless otherwise stated.

System	Electrolyte type	σ [S/cm]	Comments	Ref.
Electrospun-PEO/PAN (75:25 wt-%)	GPE	$3.7 \cdot 10^{-3}$	Electrospunmembranes, soaked in 0.5M LiI, 0.05M I_2 inPC/DEC (1:1, v/v)	[48]
Electrospun-PEO/PAN (75:25 wt-%)	GPE	$3.6 \cdot 10^{-3}$	0.5 M LiI, 0.05 M I_2 in PC/DEC (1:1, v/v)	[22]
Electrospun-PAN fibers encaculated by solution casted PEO	GPE	$1.2 \cdot 10^{-3}$	PEO including liquid $LiPF_6$	[49]
ES-multilayer PAN/PEO system	GPE	$4.7 \cdot 10^{-3}$	Multilayer composite of ES PAN; inner layer of poly (vinyl acetate) (PVAc)/poly(methyl methacrylate) (PMMA)/ poly(ethylene oxide) (PEO) fibrous membrane. Liquid electrolyte (1 M $LiPF_6$ in EC/DMC)	[50]
PEO-LiTFSI-Ionic liquid	GPE	$\approx 3 \cdot 10^{-4}$	Various ionic liquids (IL)	[51]
PAN/PEO-LiTFSI-DME/DOL/1 wt% $LiNO_3$/LATP	GPE	$8.6 \cdot 10^{-4}$	PEO/PAN 50:50 wt%, LATP, double layer GPE via casting	[52]
PEO/PAN10PEO–40PAN–12LiClO4–38EC/BL.	GPE	$1.2 \cdot 10^{-3}$	$LiClO_4$, casted, gel electrolyte in ethylene carbonate (EC) and γ-butyrolactone (BL)	[53]
PEO-PAN-LLZO in (1.0 wt% $LiNO_3$, 1 M LiTFSI DME/ DOL (1:1))	CPE/GPE	$2.0 \cdot 10^{-3}$	PEO:PAN (50:50), LLZO, (1.0 wt% $LiNO_3$, 1 ML iTFSI DME/DOL (1:1) for GPE formation	[54]
PEO SPEs including fillers like TiO_2, SiO_2, Al_2O_3, SnO_2, ZnO	CPE	10^{-4} to 10^{-5}	PEO as base polymer with various fillers and additives like EC, DEC, PVDF, LLTo, LLZAO and many others, dry, solid electrolyte	[40]
Electrospun-PEO/sodium alingate (SA) nanofiber	CPE	$6.8 \cdot 10^{-5}$ at 303 K	LiTFSI, PEGdMA, LLZTO, AIBN, and sodium alginate (SA) nanofiber additives	[55]
Electrospun-LATP/PAN in casted PEO	CPE	$6.5 \cdot 10^{-4}$	LiTFSI, LATP, PEO 600.000:LiTFSI 8:1 mass ratio	[40]
PEO/PAN hybrids	SPE, casted	$1 \cdot 10^{-10}$ to $9 \cdot 10^{-8}$	$LiClO_4$, various compositions with PEO excess	[23]
GDS NFs/PEO/LiTFSI-PAN/PVDF-1:1	SPE, casted	$2.5 \cdot 10^{-4}$	LiTFSI, PAN/PFDV electrospun fibers in casted PEO	[56]
PEO/PAN	SPE, casted	$6.79 \cdot 10^{-4}$ at 25 °C	$LiClO_4$, [EO]/[Li] ratio of about 10, and are electrochemically stable up to about 4.8 V vs Li/Li^+.	[57]
PEO/polysulfone (PSf) PEO/PSf (70:30)	SPE, casted	$3.1 \cdot 10^{-7}$ PEO/PSf (70:30)$1.8 \cdot 10^{-6}$PEO/ LiFTSI	10 wt-% LiTFSI	[58]
PAN in casted PEO-SN-LiTFSI	SPE, ES	$1.8 \cdot 10^{-4}$	PAN-PEO-(SN)x-Li10, x mass ratio of SN to PEO, Li10 PEO:Li ratio 10:1	[59]
PAN	n.a., ES	no ion conductivity	No coordination of cations within the PAN polymer.	[19]
Electrospun-PEO	SPE, ES	$1.5 \cdot 10^{-6}$	only $LiBF_4$ as conductive salt additive	[31]
PEO/SN	SPE, ES	$2 \cdot 10^{-5}$	$LiBF_4$ and SN (18:3:1)	[31]
PEO/SN	SPE, ES	$2 \cdot 10^{-4}$	$LiBF_4$ and SN (36:8:1)	[31]
PEO/PAN (50:50)	SPE, ES	$1.0 \cdot 10^{-4}$	$LiBF_4$ and SN (18:9:1)	[29]
PEO/PAN (50:50)	SPE, ES	$1.8 \cdot 10^{-5}$ to $2.5 \cdot 10^{-4}$	$LiBF_4$ and SN, various compositions	This study
PEO/PAN (50:50)	SPE, HP	$1.5 \cdot 10^{-5}$ to $1{,}8 \cdot 10^{-4}$	$LiBF_4$ and succinonitrile (SN), various compositions	This study

n.a. (not applicable), GPE (gel polymer electrolyte), CPE (combined polymer electrolyte), SPE (solid polymer electrolyte), ES (electrospun system), HP (hot-pressed), PEO (polyethylene oxide), PAN (polyacrylo nitrile), PVDF (polyvinylidene fluoride), SN (succino nitrile), PC (propylene carbonate), EC (ethylene carbonate), DEC (diethylene carbonate), LLTo (lithium lanthanum titanate), LLZO (lithium lanthanum zirconium oxide), LATP (lithium aluminum titanium phosphate, PSf (polysulfone), LiTFSI (lithium bis(trifluoromethanesulfonyl)imide) DME (dimethyle ether).

Journal of Inorganic and General Chemistry
ZAAC
Zeitschrift für anorganische und allgemeine Chemie
RESEARCH ARTICLE
15213749, 2026, 2, Downloaded from https://onlinelibrary.wiley.com/doi/10.1002/zaac.202500062 by Universitätsbibliothek Augsburg, Wiley Online Library on [05/05/2026]. See the Terms and Conditions (https://onlinelibrary.wiley.com/terms-and-conditions) on Wiley Online Library for rules of use; OA articles are governed by the applicable Creative Commons License

can only represent a small selection of the different studies reported in recent years.

PEO/PAN (50:50) SPEs reported in this study show reasonably high conductivities of $1.5 \cdot 10^{-5}$ to $2.5 \cdot 10^{-4}$ S cm^{-1} that are approximately one order of magnitude lower than the ones in GPEs where a significant amount of liquid electrolyte is present (see GPEs denoted in Table 4). The same range of conductivities (CPEs: 10^{-5} to $2 \cdot 10^{-3}$ S cm^{-1}) are observed for CPEs where either liquid electrolyte od inorganic fillers are added to improve the conductivity. Most important the observed conductivities overcome or reach most of the casted SPEs (casted, dry SPEs: 10^{-10} to 6.5 10^{-4} S cm^{-1}). Taking a closer look to electrospun pure PEO and PEO/PAN systems, the incorporation of PAN as a matrix to host the ion conducting PEO phase does not influence the overall ion conductivity of the system. Both conductivities are literally identical. A mechanism for this ion transport through an ES PEO/PAN membrane including differential scanning calorimetry (DSC) was reported earlier on.[29] In principle, ion conduction is preferred and accelerated on the surface of the ES PEO fibers, and reasonable contacts are present between the aligned and neighbored PEO fibers to allow ion transport in all directions. The same principle seems to be valid for the hot-pressed samples in this study since the conductivity is literally identical with the ES ones.

3. Conclusion

Mixed PAN/PEO polymer electrolytes were synthesized following either the electrospinning (ES) or the hot-pressing (HP) approach. Succinonitrile and—in the case of the ES samples—propylene carbonate were added as plasticizers. While the ES samples offer a favorable interwoven fiber structure which has been shown to enhance ion mobility in these sample, the resulting composition of the ES membranes, especially in relation to the plasticizer content was observed to spread considerably, in some cases resulting in a complete loss of the plasticizer added to the starting mixture. Cation, anion, and PEO segmental chain mobility, as determined from temperature dependent ^{7}Li-, ^{19}F-, and ^{13}C-NMR, were found to correlate quite well with the plasticizer content. No PAN dynamics was observed; its role seems to be limited to increase the mechanical stability of the membranes.

For the HP processed samples, we found a decent correlation between target and actual compositions. Hence, for the HP samples, the influence of compositional parameters (PEO/plasticizer ratio and PEO/PAN ratio) on the membranes' performance was studied. The presence of SN clearly suppresses the crystallization tendency for PEO and the PEO_3:$LiBF_4$ complex; PAN is found to aid in the suppression of PEO crystallization. Again, a straight correlation could be observed between plasticizer content (SN) and activation energy for anion and cation mobility. Thus, the presence of SN enhances the ion mobility in two ways, not only acting as a lubricant to enhance chain mobility but moreover increasing the amount of amorphous PEO in the membranes. Varying the PEO/PAN ratio did not entail any change in the membranes' dynamics; PAN is found immobile in the samples, mainly serving to enhance the dimensional stability of the membranes and thus counterbalance the detrimental effect of the addition of SN without deteriorating the ion mobility. Sample HP8, a PEO-free PAN:SN:$LiBF_4$ membrane showed unexpected high ionic conductivity and mobility. For all PEO-containing samples, coordination of Li by the ether oxygen is expected as the dominating coordination motif, with only limited participation of SN; for the PEO-free sample, the formation of $Li^{+}(SN)_x$ moieties acting as a vehicle for Li transportation seems probable and is supported by the matching ^{7}Li chemical shift as compared to work by Voigt et al.[20] The first assumption has been supported by ^{7}Li {^{1}H} constant time REDOR experiments performed on samples HP1 and HP1-d4 (synthesized using fully deuterated SN). The virtual identical REDOR curves for these samples suggest that SN is not playing any extended role in Li coordination. Experiments to unravel more details of the mechanism of Li ion migration in the studied samples—these include ^{7}Li-^{13}C dipolar experiments with cross-polarizing magnetization from ^{1}H to ^{13}C at low temperatures will be possible in our laboratories in the near future and are expected to work out the subtle differences in the mechanism of ion conduction in PAN and PEO based electrolyte membranes.

4. Experimental Section

$LiBF_4$ was chosen as a conductive salt additive because of its moisture stability and ability to be handled on air. This was important for all samples that have been fabricated via electrospinning in this study. In order to compare casted and electrospun samples, we kept the conductive salt identical in all systems.

Fabrication of Membranes via Electrospinning (ES): Five samples ES1 to ES5 were prepared using the following procedure. The polymer solutions were prepared in a glovebox in a dry inert atmosphere ($O_2 < 0.1$ ppm, $H_2O < 0.1$ ppm) using snap-on cap glassware with magnetic stirring. In the first step, PAN (Sigma Aldrich, 150 000 g mol^{-1}) was added to the snap-on cap glass and was then dissolved in DMSO (dimethyl sulfoxide). Subsequently, the plasticizer propylene carbonate (PC) was added. The reactants were stirred until a homogeneous solution was achieved, after which a specified amount of MeCN (acetonitrile) was added. Subsequently, PEO (Sigma Aldrich, 300 000 g mol^{-1}) and SN were added to the solution. The mixture was stirred overnight. The conductive salt $LiBF_4$ was added 2 h before the electrospinning process was initiated. Five different batches, all aiming at the same target composition of 10 PEO : 8 PAN : 5 SN : 4 PC, were prepared (each starting mixture consisted of 0.175 g PEO, 0.175 g PAN, 0.150 g SN, 0.168 g PC, and 0.0367 g $LiBF_4$, with 3 mL DMSO and 2 mL MeCN as solvents). The spinning process then was performed in the laboratory, and the membranes were then dried afterwards for 24 h in a desiccator on a Schlenk line. During electrospinning, a voltage of 18 to 20 kV was applied. The distance between the tip of the cannula and the grounded collector averaged 20 cm, and the solution was pumped at a feed rate of 1.5–3 mL per hour.

Fabrication of Membranes via Hot-Pressing (HP): To facilitate processing of succinonitrile (SN), which exhibits a quite sticky texture at room temperature, SN was embrittled by cooling down with liquid nitrogen and then subsequently crushed in an agate mortar and then dried for several days at room temperature. The remaining starting materials were dried under vacuum for several days. The reactants were stored in the glove box in an argon atmosphere until further processing. In a first step, mixtures according to the quantities listed in Table S1_a, supporting information, were homogenized using a ball mill. The reactants were transferred to the filling containers of the planetary mill in an argon box and the vessels sealed with

parafilm to minimize uptake of water. For the milling process, 5 min of milling (400 rpm) were followed by 5 min of resting for 16 h in toto. The resulting mixtures were then transferred to the press template—sandwiched by Mylar film to ease removal—in argon atmosphere. The pressing process was carried out at a temperature of 100 °C at 5 T pressure over a period of 20 °min. The pressing template was then cooled to room temperature using a copper block. The membranes were removed from the press template and stored in an argon atmosphere.

X-Ray Diffraction: The crystallinity of all samples was assessed via powder X-ray diffraction using a Guinier powder diffractometer using Cu-$K_{\alpha 1}$ radiation ($\lambda = 1.54051$ Å). The equipment was operated with a G670 Imaging-Plate-Detector. The measurement was conducted between 10 and 80° (2θ). A portion of the membranes was placed between two PET films with a thickness of 6 μm in a flat-bed sample holder. All measurements were performed at room temperature.

Potentiostatic Electrochemical Impedance Spectroscopy (PEIS): The impedance analysis was operated with a Metrohm Autolab B.V. PGSTAT204 potentiostat including an FRA 32 *M* module and a cell setup by rhd with a TSC standard battery cell with stainless steel nickel-plated electrodes. The membranes were punched out in the shape of a disc with a 10 mm-diameter and placed between the electrodes and placed between the stainless steel electrodes. The measurement area a was 0.50265 cm^2. PEIS data was collected using an amplitude of 20 mV, in the frequency range of 1 MHz to 0.1 Hz, at temperatures from 293 to 328 K in steps of 5 K. The thickness d of the samples was determined after the measurements with a micrometer screw (Holex, 0–25 mm, 0.001 mm accuracy). The thickness of the membranes varied between 40 and 114 μm for the ES and between 80 and 467 μm for the HP samples. Conductivities were calculated using the equation $\sigma = (1/R)\cdot(d/a)$ where the resistance (R), the thickness (d), and the area (a) where taken into account. We assumed full contact to the electrodes neglecting the tortuosity and lower contact area of the fiber membranes to the electrodes. The resulting Nyquist plots were analyzed using the RelaxIS 3 software by rhd instruments. Selected Nyquisit plots are given in the supplement section.

NMR Spectroscopy: The solid-state nuclear magnetic resonance experiments were conducted using a BRUKER Avance III spectrometer in combination with a 7 T magnet at resonance frequencies of 46.1 MHz, 75.5 MHz, 116.6 MHz, 282.5 MHz, and 300 MHz for ^2H, ^{13}C, ^7Li, ^{19}F, and ^1H. 4 mm WVT MAS triple and double resonance probes were used in combination with 4 mm ZrO_2-rotors. All preparation steps were performed in an argon-filled glovebox, and the measurements were performed using a nitrogen flow. A heat exchanger in combination with liquid nitrogen was used for the low temperature measurements with the temperature being calibrated using $Pb(NO_3)_2$ as a chemical shift thermometer.[43,44]

^7Li and ^{19}F static single pulse experiments were conducted within a temperature range of 171 K to 360 K to obtain information about the cation and anion dynamics. MAS experiments were performed at 10 kHz. Relaxation delays between 5 s and 60 s, depending on the measurement temperature, were used.

^{13}C-MAS experiments and ^{13}C-{^1H}-CP-MAS-experiments in the temperature range from 178 K to 328 K and relaxation delays of 10 s to 300 s were performed to obtain information about PEO and PAN dynamics. For the CP-MAS experiments, the contact time was varied between 0.1 ms and 8 ms.

^7Li-{^1H}-constant time REDOR NMR was performed to check whether in the PEO-containing samples SN is contributing significantly to the local Li coordination. For this, the results from two samples with identical composition, HP1 and HP1-d4, in which in HP1-d4 fully deuterated succinonitrile was used for the synthesis, were compared. These experiments were performed at the lowest accessible temperature of 190 K to guarantee the freezing of all motional processes.

To evaluate the compositions of the samples, ^{13}C-MAS NMR with high power ^1H decoupling was used to evaluate the composition of the samples. A relaxation delay of 300 s was used to assure complete relaxation of the ^{13}C nuclei. The spectra were then fitted using the program DMFIT[45] to obtain the relative amounts of PEO, PAN, SN, PC, and DMSO. Details of the analysis are given in the supporting information.

In addition, the compositions were determined analyzing the ^1H NMR signals on samples dissolved in DMSO-d6 using ^1H solution-state NMR using a 400 MHz Varian Mercury plus NMR spectrometer.

Acknowledgements

This work was founded by the DFG under grants Ni1095/9-1 and WU237/9-1 and is part of the project "Industrialisierbarkeit von Festkörperelektrolytzellen" funded by the Bavarian Ministry of Economic Affairs, Regional Development and Energy. The conduction of SEM measurements by Katia Rodewald at the Wacker Chair of Macromolecular Chemistry and Dr. Maximilian Winkler from the Chair of Experimentalphysik V are gratefully acknowledged. Further thanks go to Elisabeth Springl for the impedance measurement. Anna Kirchberger thanks the TUM Graduate School for support.

Open Access funding enabled and organized by Projekt DEAL.

Conflict of Interest

The authors declare no conflict of interest.

Data Availability Statement

The data that support the findings of this study are available from the corresponding author upon reasonable request.

Keywords: all-solid-state batteries · electro-spinning · hot-pressing · lfp battery · NMR spectroscopy · solid polymer electrolytes

[1] Q. Wang, P. Ping, X. Zhao, G. Chu, J. Sun, C. Chen, *J. Power Sources* **2012**, *208*, 210.
[2] L. B. Diaz, X. He, Z. Hu, F. Restuccia, M. Marinescu, J. V. Barreras, Y. Patel, G. Offer, G. Rein, *J. Electrochem. Soc.* **2020**, *167*, 090559.
[3] P. Knauth, *Solid State Ion.* **2009**, *180*, 911.
[4] Z. Zhang, S. S. Zhang, *Rechargeable Batteries*, Springer International Publishing, Cham **2015**.
[5] D. Golodnitsky, E. Strauss, E. Peled, S. Greenbaum, *J. Electrochem. Soc.* **2015**, *162*, A2551.
[6] K. S. Ngai, S. Ramesh, K. Ramesh, J. C. Juan, *Ionics (Kiel).* **2016**, *22*, 1259.
[7] F. B. Dias, L. Plomp, J. B. J. Veldhuis, *J. Power Sources* **2000**, *88*, 169.
[8] A. M. Stephan, K. S. Nahm, *Polymer (Guildf).* **2006**, *47*, 5952.
[9] P. Yao, H. Yu, Z. Ding, Y. Liu, J. Lu, M. Lavorgna, J. Wu, X. Liu, *Frontiers Chem.* **2019**, *7*, 522.
[10] A. Manthiram, X. Yu, S. Wang, *Nature Rev. Mater.* **2017**, *2*, 16103.

[11] A. Arya, A. L. Sharma, *J. Mater. Sci.* **2020**, *55*, 6242.
[12] P. V. Wright, *Electrochim. Acta* **1998**, *43*, 1137.
[13] D. E. Fenton, J. M. Parker, P. V. Wright, *Polymer (Guildf.)*. **1973**, *14*, 589.
[14] M. Armand, M. Duclot, P. Rigaud, *Solid State Ion.* **1981**, *3-4*, 429.
[15] W. Liu, N. Liu, J. Sun, P.-C. Hsu, Y. Li, H.-W. Lee, Y. Cui, *Nano Lett.* **2015**, *15*, 2740.
[16] N. Wu, P.-H. Chien, Y. Li, A. Dolocan, H. Xu, B. Xu, N. S. Grundish, H. Jin, Y.-Y. Hu, J. B. Goodenough, *J. Am. Chem. Soc.* **2020**, *142*, 2497.
[17] P. Walke, A. Kirchberger, F. Reiter, D. Esken, T. Nilges, *Z. Naturforsch. B.* **2021**, *76*, 615.
[18] N. Voigt, L. van Wüllen, *Solid State Ion.* **2014**, *260*, 65.
[19] N. Voigt, L. van Wüllen, *Solid State Ion.* **2012**, *208*, 8.
[20] N. Voigt, *Neue Einblicke in den Ionentransport Polymer-basierter Lithium-Hybridelektrolyte mithilfe der Festkörper-NMR-Spektroskopie, Dissertation*, University Münster **2013**.
[21] B. K. Choi, Y. W. Kim, H. K. Shin, *Electrochim. Acta* **2000**, *45*, 1371.
[22] S. Abdollahi, H. Sadadi, M. Ehsani, E. Aram, *Ionics (Kiel).* **2021**, *27*, 3477.
[23] W. Chun-Guey, W. Chiung-Hui, L. Ming, I. C. Huey-Jan, *J. Appl. Polymer Sci.* **2006**, *99*, 1530.
[24] S. Rajendran, *Solid State Ion.* **2000**, *130*, 143.
[25] G. B. Appetecchi, J. Hassoun, B. Scrosati, F. Croce, F. Cassel, M. Salomon, *J. Power Sources* **2003**, *124*, 246.
[26] G. B. Appetecchi, F. Croce, J. Hassoun, B. Scrosati, M. Salomon, F. Cassel, *J. Power Sources* **2003**, *114*, 105.
[27] L. Wang, X. Li, W. Yang, *Electrochim. Acta* **2010**, *55*, 1895.
[28] L. Zhao, M. Hou, K. Ren, D. Yang, F. Li, X. Yang, Y. Zhou, D. Zhang, S. Liu, Y. Lei, F. Liang, *Small Methods* **2024**, *8*, e2301579.
[29] A. M. Kirchberger, P. Walke, J. Venturini, T. Nilges, *Membranes* **2025**.
[30] K. M. Freitag, P. Walke, T. Nilges, H. Kirchhain, R. J. Spranger, L. van Wüllen, *J. Power Sources* **2018**, *378*, 610.
[31] K. M. Freitag, H. Kirchhain, L. van Wüllen, T. Nilges, *Inorg. Chem.* **2017**, *56*, 2100.
[32] P. Walke, K. M. Freitag, H. Kirchhain, M. Kaiser, L. van Wüllen, T. Nilges, *Z. Anorg. Allg. Chem.* **2018**, *644*, 1863.
[33] J. Waugh, E. I. Fedin, *Sov. Physics-Solid State* **1963**, *4*, 1633.
[34] C. Berthier, W. Gorecki, M. Minier, M. B. Armand, J. M. Chabagno, P. Rigaud, *Solid State Ion.* **1983**, *11*, 91.
[35] J. J. Dechter, *J. Polymer Sci.: Polymer Lett. Ed.* **1985**, *23*, 261.
[36] A. Johansson, J. Tegenfeldt, *Macromolecules* **1992**, *25*, 4712.
[37] H. Kirchhain, in *Dissertation*, Universität Augsburg **2021**.
[38] T. Echelmeyer, L. van Wüllen, S. Wegner, *Solid State Nucl. Magn. Res.* **2008**, *34*, 14.
[39] T. Echelmeyer, S. Wegner, L. van Wüllen, G.A. Webb, *Annual Reports on NMR Spectroscopy* **2012**, *75*, 1–23.
[40] X. Li, Y. Deng, K. Li, Z. Yang, X. Hu, Y. Liu, Z. Zhang, *Polymers (Basel).* **2023**, *15*, 3727.
[41] R. Whba, M. S. Su'ait, F. Whba, A. Ahmad, *J. Power Sources* **2024**, *606*, 234539.
[42] D. Zhang, L. Li, X. Wu, J. Wang, Q. Li, K. Pan, J. He, *Front. Energy Res.* **2021**, *9*, 726738.
[43] A. Bielecki, D. P. Burum, *J. Magn. Res., Series A.* **1995**, *116*, 215.
[44] T. Takahashi, H. Kawashima, H. Sugisawa, T. Baba, *Solid State Nucl. Magn. Res.* **1999**, *15*, 119.
[45] D. Massiot, F. Fayon, M. Capron, I. King, S. L. Calvé, B. Alonso, J.-O. Durand, B. Bujoli, Z. Gan, G. Hoatson, *Magn. Res. Chem.* **2002**, *40*, 70.
[46] Y. G. Andreev, V. Seneviratne, M. Khan, W. A. Henderson, R. E. Frech, P. G. Bruce, *Chem. Mater.* **2005**, *17*, 767.
[47] S. M. Zahurak, M. L. Kaplan, E. A. Rietman, D. W. Murphy, R. J. Cava, *Macromolecules* **1988**, *21*, 654.
[48] S. Abdollahi, M. Ehsani, J. Morshedian, H. A. Khonakdar, U. Reuter, *Polymer Comp.* **2018**, *39*, 3377.
[49] W. U. Arifeen, B. Akkinepally, Z. U. Abideen, I. Hussain, M. R. Siddiqui, S. Li, J. Shim, T. J. Ko, *J. Industrial Engin. Chem.* **2025**, *142*, 746.
[50] D.-H. Lim, A. Haridas, S. P. Anupriya, P. Figerez, A. Raghavan, A. Matic, J.-H. Ahn, *J. Nanosci. Nanotechnol.* **2018**, *18*, 6499.
[51] G. P. Pandey, Y. Kumar, S. A. Hashmi, *Indian J. Chem.* **2010**, *49*, 743.
[52] X. Wang, X. Hao, Y. Xia, Y. Liang, X. Xia, J. Tu, *J. Membrane Sci.* **2019**, *582*, 37.
[53] B. K. Choi, Y. W. Kim, H. K. Shin, *Electrochim. Acta* **2000**, *5*, 1371.
[54] P. Xie, R. Yang, Y. Zhou, B. Zhang, X. Tian, *Chem. Engin. J.* **2022**, *450*, 138195.
[55] Q. Sun, Z. Liu, P. Zhu, P. J. J. Liu, S. Shang, *Energies (Basel).* **2023**, *16*, 5819.
[56] N. Deng, S. Luo, L. Zhang, Y. Feng, Y. Liu, W. Kang, B. Cheng, *J. Energy Storage* **2024**, *75*, 109578.
[57] F. Yuan, H.-Z. Chen, H.-Y. Yang, H.-Y. Li, M. Wang, *Mater. Chem. Phys.* **2025**, *89*, 390.
[58] F. Gucci, M. Grasso, C. Shaw, G. Leighton, V. M. Rodriguez, J. Brighton, *Polymer-Plastics Techn. Mater.* **2023**, *62*, 1019.
[59] Y. Zhang, H. Wang, Y. Yang, J. Xie, Q. Deng, W. Zou, A. Zhou, J. Li, *Chem. Engin. J.* **2023**, *461*, 141993.

Manuscript received: March 28, 2025
Revised manuscript received: August 19, 2025
Version of record online: November 17, 2025